Geochemical Perspectives Letters

Early precipitated micropyrite in microbialites: A time capsule of microbial sulfur cycling

J. Marin-Carbonne[1*], M.-N. Decraene[1], R. Havas[2], L. Remusat[3], V. Pasquier[4], J. Alléon[1], N. Zeyen[5], A. Bouton[2], S. Bernard[3], S. Escrig[6], N. Olivier[7], E. Vennin[2], A. Meibom[6,1], K. Benzerara[3], C. Thomazo[2,8]

https://doi.org/10.7185/geochemlet.2209

Abstract

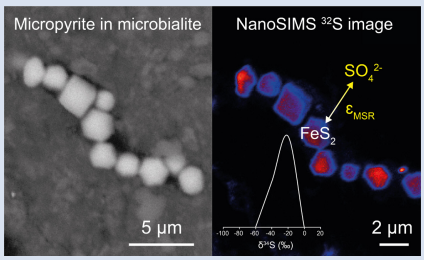

Microbialites are organosedimentary rocks that have occurred throughout the Earth's history. The relationships between diverse microbial metabolic activities and isotopic signatures in biominerals forming within these microbialites are key to understanding modern biogeochemical cycles, but also for accurate interpretation of the geologic record. Here, we performed detailed mineralogical investigations coupled with NanoSIMS (Nanoscale Secondary Ion Mass Spectrometry) analyses of pyrite S isotopes in mineralising microbial mats from two different environments, a hypersaline lagoon (Cayo Coco, Cuba) and a volcanic alkaline crater lake (Atexcac, Mexico). Both microbialite samples contain two distinct pyrite morphologies: framboids and euhedral micropyrites, which display distinct ranges of $\delta^{34}S$ values[1]. Considering the sulfate-sulfur isotopic compositions associated with both environments, micropyrites display a remarkably narrow range of Δ_{pyr} (*i.e.* $\Delta_{pyr} \equiv \delta^{34}S_{SO_4} - \delta^{34}S_{pyr}$) between 56 and 62 ‰. These measured Δ_{pyr} values agree with sulfate-sulfide equilibrium fractionation, as observed in natural settings characterised by low microbial sulfate reduction respiration rates. Moreover, the distribution of S isotope compositions recorded in the studied micropyrites suggests that sulfide oxidation also occurred at the microbialite scale. These results highlight the potential of micropyrites to capture signatures of microbial sulfur cycling and show that S isotope composition in pyrites record primarily the local micro-environments induced by the microbialite.

Received 21 October 2021 | Accepted 14 February 2022 | Published 21 March 2022

Introduction

Sulfate-reducing bacteria, *i.e.* microorganisms that use sulfate as a terminal electron acceptor, are ubiquitous in Earth environments where they play a major role both in S and C biogeochemical cycles (*e.g.*, Jørgensen *et al.*, 2019). Microbial sulfate reduction (MSR) reduces sulfate to dissolved S species, such as HS^- and H_2S, and discriminates against heavy sulfur isotopes. The resulting sulfide $\delta^{34}S$ values are relatively light and can be as much as −70 ‰ relative to sulfate (Jørgensen *et al.*, 2019). The fractionation induced by this metabolic activity ($^{34}\varepsilon_{mic}$ hereafter) depends on the sulfate concentration, identity of the electron donor, bioavailable carbon (content and chemical form) and, perhaps most importantly, the cell-specific sulfate reduction rates (csSRR; Bradley *et al.*, 2016). In modern environments, MSR can be identified by rate measurements with radiotracers or genomic and proteomic approaches. However, since genetic markers are not preserved in the geological record, the recognition of MSR in palaeoenvironments mostly relies on the sulfur isotopic compositions of sedimentary sulfide and sulfate minerals (Visscher *et al.*, 2000; Fike *et al.*, 2008).

MSR plays a key role in carbonate mineralisation, especially identified in microbialites and microbial mats (Visscher *et al.*, 2000). Microbial mats are stratified microbial communities whose metabolic activities produce geochemical gradients and drive elemental cycling (Canfield and Des Marais, 1993; Paerl and Pinckney, 1996). In the geological record, such deposits (often referred to as stromatolites) are considered among the oldest trace of life on Earth (Allwood *et al.*, 2009). Some Archaean stromatolites contain carbonaceous laminae that have been interpreted as fossil microbial mats or biofilms based on textural evidence (Awramik, 1992; Lepot, 2020). Interestingly, determining the precise nature of the fossil microbial community

1. Institute of Earth Sciences, Université de Lausanne, Geopolis, Mouline 1015 Lausanne, Switzerland
2. UMR CNRS/uB6282 Biogéosciences, UFR Science Vie Terre Environnement, Université de Bourgogne Franche Comté, Dijon, France
3. Muséum National d'Histoire Naturelle, Sorbonne Université, CNRS UMR7590, Institut de Minéralogie, de Physique des Matériaux et de Cosmochimie (IMPMC), Paris, France
4. Earth and Planetary Sciences, Weizmann Institute of Sciences, Rehovot, Israel
5. Department of Earth and Atmospheric Sciences, University of Alberta, T6G 2E3, Canada
6. Laboratory for Biological Geochemistry, School of Architecture, Civil and Environmental Engineering, Ecole PolytechniqueFédérale de Lausanne, CH-1015 Lausanne, Switzerland
7. Université Clermont Auvergne, CNRS, IRD, Laboratoire Magmas et Volcans, F-63000 Clermont-Ferrand, France
8. Institut Universitaire de France, Paris, France
* Corresponding author (email: johanna.marincarbonne@unil.ch)

[1] $\delta^{34}S = ((^{34}S/^{32}S)_{sample}/(^{34}S/^{32}S)_{reference} - 1) \times 1000$ in ‰, with Vienna Canyon Diablo Troilite as the reference.

is challenging because these organosedimentary rocks resulted from a complex balance between microbial activities, sedimentation and intermittent lithification (Reid *et al.*, 2000). In addition, the biosignatures preserved in fossil biofilms are ambiguous, especially after diagenesis and post-depositional history (Javaux, 2019; Alleon *et al.*, 2021). The oldest evidence for MSR in the Archaean geological record are sulfur isotopic signatures from deep marine sediments (Kamber and Whitehouse, 2007; Shen *et al.*, 2009) and stromatolites (Shen and Buick, 2004). In modern microbialites, numerous studies have reported dynamic MSR activity based on H_2S labelling (Visscher *et al.*, 2000; Fike *et al.*, 2008; Pace *et al.*, 2018; Gomes *et al.*, 2021), but only a few studies have investigated sulfur isotope signatures of individual pyrite grains (Gomes *et al.*, 2021).

The primary S isotopic signatures of pyrites (FeS_2) are often modified by fluid circulation during metasomatism or metamorphism (Marin-Carbonne *et al.*, 2020; Slotznick *et al.*, 2022), occurring millions or billions of years after sediment deposition. While late diagenesis can modify both pyrite crystallinity and S isotope composition (Williford *et al.*, 2011; Gomes *et al.*, 2018; Marin-Carbonne *et al.*, 2020), early diagenesis in microbial mats is thought to have a limited effect on the S isotopic composition of pyrite, meaning that microbialitic pyrites may preserve 'pristine' isotopic signatures. However, the observation of large isotopic differences of about ~30 ‰ (Raven *et al.*, 2016) between pore water sulfur species (SO_4^{2-} and H_2S) and pyrite shows that other S-bearing pools, such as organic matter, should be considered in order to quantitatively and isotopically describe sulfur cycling in microbialites. Pyrite often precipitates at the microbial mat surface (Gomes *et al.*, 2021) and its isotopic composition is more representative of the local setting rather than global environmental conditions, *e.g.*, water column (Lang *et al.*, 2020; Pasquier *et al.*, 2021). Decoding pyrite S isotopes at the microscale in sedimentary rocks is required to better understand how local conditions may affect the isotopic composition of microbialite pyrites. Here, we focus our investigation on two geographically independent modern microbial mats, which have not yet undergone (complete) lithification, and/or metasomatism.

Syngenetic Microbialitic Pyrites

We studied two samples from 1) the Atexcac Lake, a monomictic volcanic crater lake (Mexico; Zeyen *et al.*, 2021) and 2) Cayo Coco Lake, a shallow hypersaline lagoon in Cuba (Pace *et al.*, 2018; Bouton *et al.*, 2020). These two depositional settings exhibit contrasting water column sulfate concentrations of 2.1 and 62 mM for Lake Atexcac and Cayo Coco, respectively (Figs. S-1 and S-2, SI). Both samples were produced by mineralising microbial mats and contained authigenic aragonite, Mg-rich calcite, dolomite, authigenic hydrated Mg-silicates/silica such as kerolite, and detrital phases such as feldspars and illite (Figs S-1 and S-2, SI). In each locality, pyrite morphologies fall into two different categories (Fig. 1): framboidal pyrites, ranging from 3 to 15 µm, and mono-crystal pyrites of a few micrometres (>3 µm), hereafter called micropyrites (Figs. 1 and 2, SI). Transmission electron microscopy analyses revealed an early origin of the micropyrite grains (SI). Considering both the

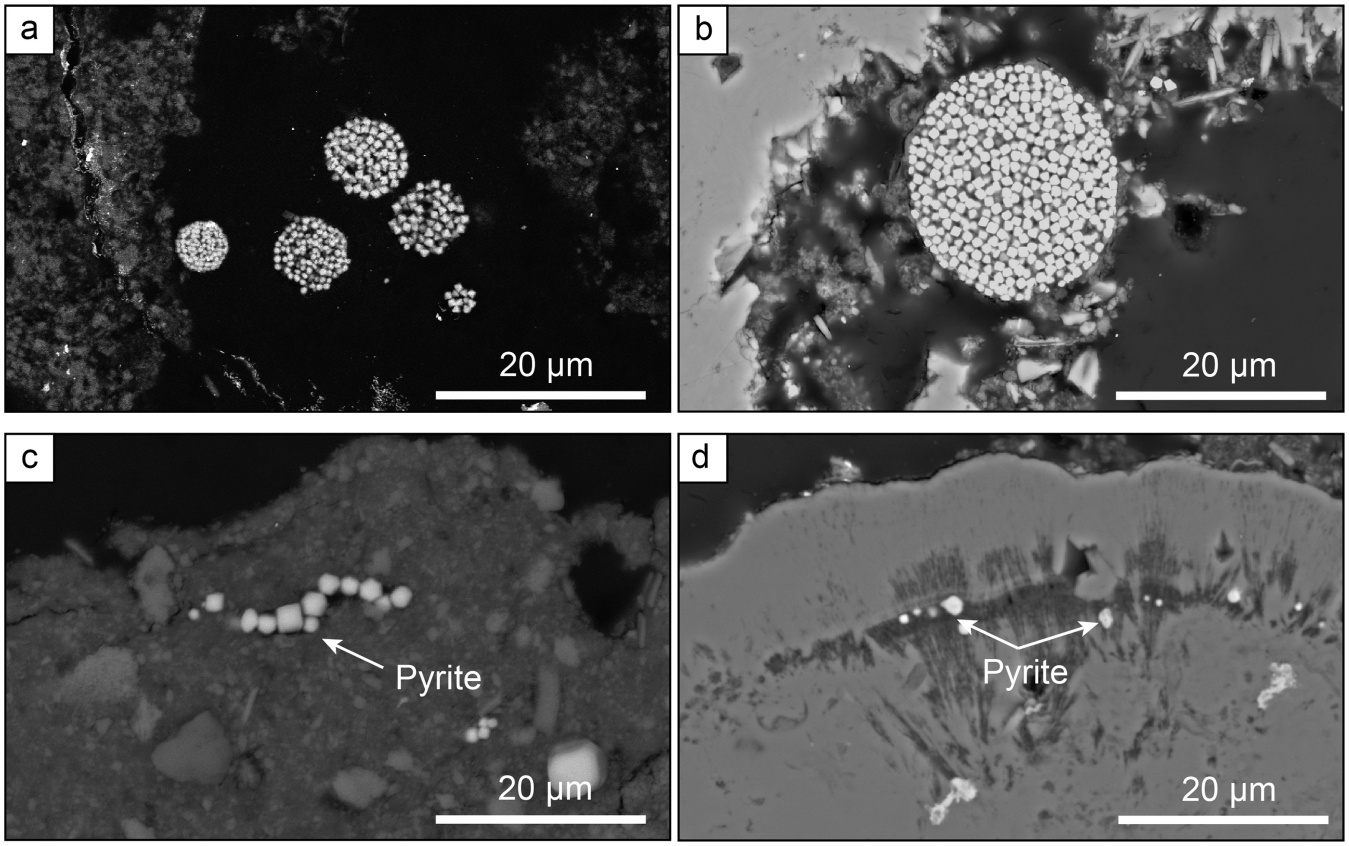

Figure 1 Secondary Electron microscopy pictures of **(a, b)** framboidal pyrites and **(c, d)** micropyrites from **(a, c)** Cayo Coco Lagoon and **(b, d)** Atexcac. Framboidal pyrites are located at the surface of the mineralised microbialite (in dark) while micropyrites are entombed within aragonite (in light grey) or Mg rich silicate (dark grey).

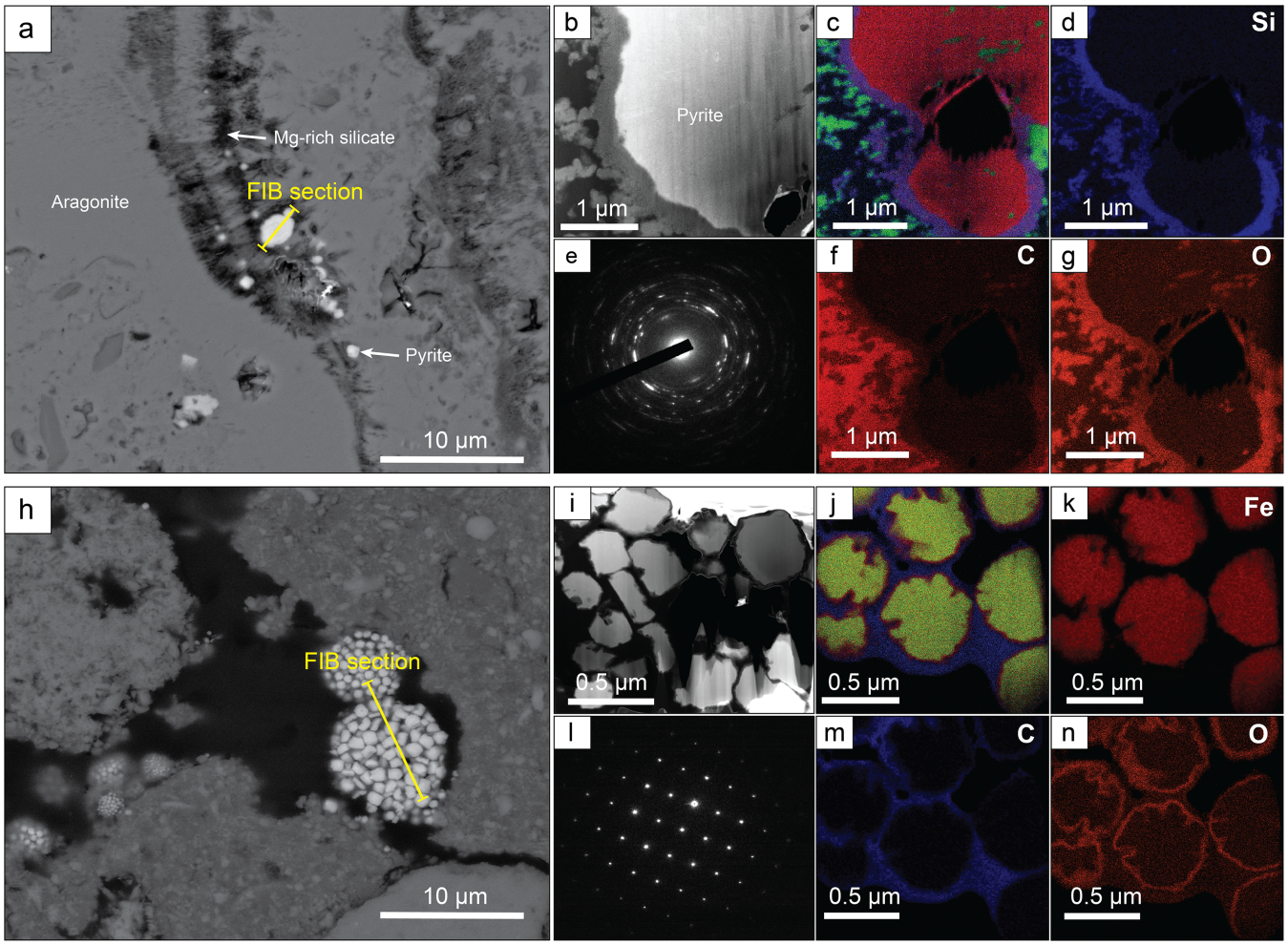

Figure 2 **(a)** SEM picture of micropyrites. Location where FIB section was extracted is shown by the yellow line, **(b)** TEM picture of the pyrite crystal and **(e)** its associated powder-like diffraction pattern, **(c)** false colour STEM EDXS image (Si in blue, Ca in green, Fe in red) and **(d, f, g)** Si, C and O images of the submicrometric pyrites, respectively. **(h)** SEM picture of framboidal pyrite with FIB section location (yellow line), **(i)** TEM image and **(l)** associated single crystal diffraction pattern along the [112] zone axis of pyrite, **(j)** false colour STEM EDXS image of pyrite crystallites (Fe in red, S in green, C in blue) and **(k, m, n)** Fe, C and O images, respectively.

alignment of the micropyrites within the organic lamination and their crystallinity, micropyrites are likely formed during an early lithification stage (SI).

NanoSIMS S Isotope Composition of Pyrites

The S isotope compositions of 66 framboidal pyrites and 55 individual micropyrites were measured by NanoSIMS with a reproducibility better than 2 ‰ (2σ, see SI). Framboidal pyrites display a ~20–30 ‰ range in $\delta^{34}S$ values with an average of −26.1 ± 7 ‰ and −26.4 ± 9 ‰ (2 s.d.) for Atexcac and Cayo Coco, respectively (Figs. 3 and 4). We have extracted S isotope composition of individual crystallites from four framboids (Fig. 3, SI). All framboidal pyrites (n = 4) show a large internal $\delta^{34}S$ variability (~40 ‰, Fig. 3) characterised by a gradient from ~+8.5 ± 1.5 ‰ to more ^{34}S-depleted values ranging from −42 to −69 ‰. Micropyrites also show large S isotope heterogeneities with $\delta^{34}S$ values ranging from −86 to −17 ‰ with an average value of −61.4 ± 17 ‰ for Atexcac, and from −53 to −21 ‰ with an average value of −34.5 ± 29 ‰ in Cayo Coco (Fig. 4).

Framboidal Pyrites Record a Mixing of Reduction and Oxidation Processes

Framboidal pyrites display a large range of $\delta^{34}S$ values but also an internal isotope variation across the length scale of individual framboidal grains (Fig. 3), best explained by a combination of MSR and partial sulfide oxidation (Fig. 3; Pellerin *et al.*, 2019). As framboidal pyrites are mostly observed at the surface of the mat, S isotope variations reflect the mixing of in situ production, upward diffusion of sulfide in the mat and its subsequent reoxidation at the mat surface. The fractionation required to produce such an isotopic gradient is well above abiotic sulfide oxidation (*i.e.* ~+5 ‰; Fry *et al.*, 1988), yet can also be consistent with microbial sulfide oxidation in high pH environments (Pellerin *et al.*, 2019). Both sites are characterised by high pH (pH > 8, see SI), which is known to promote large isotope fractionation during sulfide oxidation (Pellerin *et al.*, 2019). Consequently, part of the observed range of $\delta^{34}S$ values may be attributed to local variation of S speciation associated with pH. As such, the internal gradient may be the result of microbially mediated surface H_2S oxidation. Alternatively, the internal isotope gradient across the framboidal pyrites (Fig. 2, SI) can be due to Rayleigh isotope fractionation, as even under

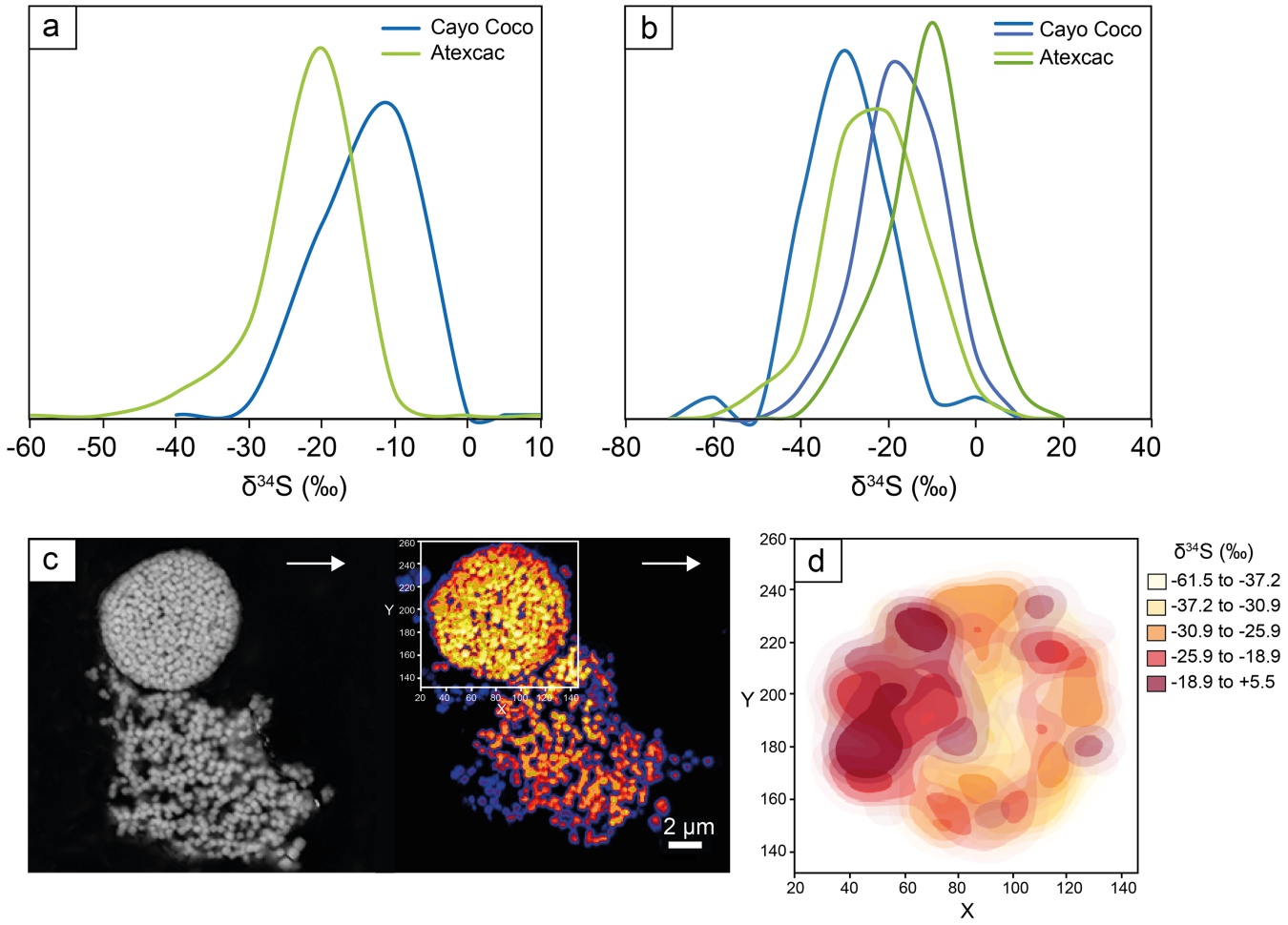

Figure 3 **(a)** $\delta^{34}S$ probability density function of all framboidal pyrites from Atexcac and Cayo Coco uncertainties of analyses ranges from 0.4 to 4 ‰, **(b)** $\delta^{34}S$ probability density function of four individual framboidal pyrites containing up to 100 pyrite crystallites, **(c)** SEM and corresponding NanoSIMS ^{32}S image of one framboidal pyrite; the arrow indicates the top of the mat, and **(d)** $\delta^{34}S$ values reconstructed for individual pyrite crystallites showing strong variations in S isotope composition across the framboidal pyrite.

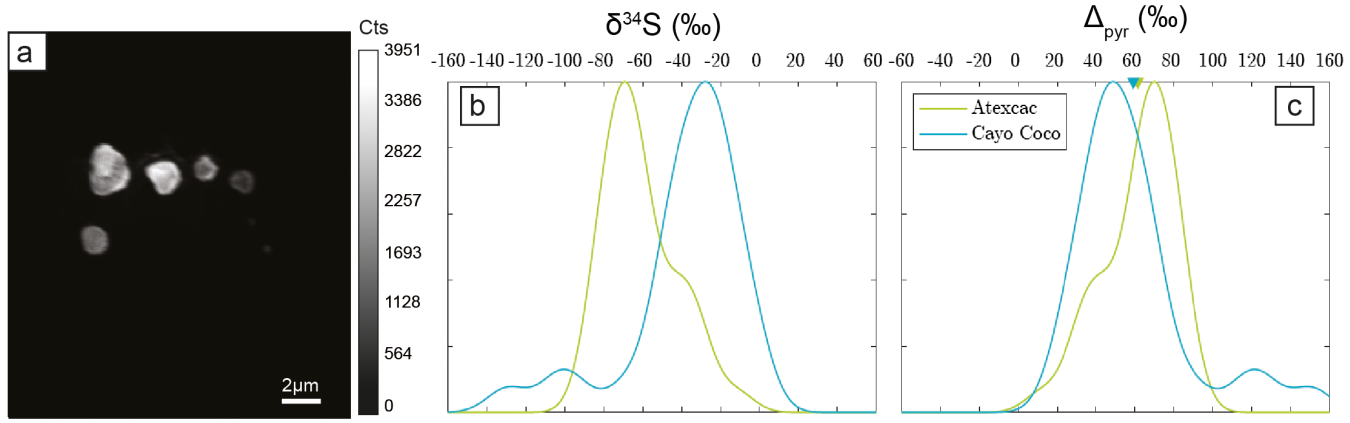

Figure 4 **(a)** NanoSIMS ^{32}S image of submicrometric pyrites, **(b)** $\delta^{34}S$ probability density function, taking account of the range of uncertainties from 1 ‰ to 8 ‰ of micropyrites from Cayo Coco and Atexcac, **(c)** Δ_{pyr} distribution calculated for both environments.

oxidising (abundant sulfate) conditions, consumption can occur faster than diffusive replenishment (Goldhaber and Kaplan, 1980). Rather than reflecting water column conditions, the S isotope composition of framboidal pyrites appears to be strongly influenced by local redox conditions (*i.e.* at the microbial mat scale).

Microbialitic Micropyrite Preserve Primary Isotopic Microbial Fractionation Signatures

The presence of Mg silicate rich rims (SI) suggests that micropyrites were probably formed very early during lithification (Fig. 2). Moreover, the small crystal size of micropyrites composed of nanocrystals with different orientations has been highlighted as a possible biogenic signature (Picard *et al.*, 2018). The $\delta^{34}S$ values of dissolved sulfate are +0.52 ‰ in Atexcac and are assumed to be close to seawater composition (+21 ‰) for Cayo Coco (SI). Considering these hugely contrasting isotopic compositions of sulfate, micropyrites display surprisingly similar Δ_{pyr} values (*i.e.* $\Delta_{pyr} = \delta^{34}S_{SO_4} - \delta^{34}S_{pyr}$) of 61.4‰ ± 18.3‰ and 59.1‰ ± 29.6‰ for Atexcac and Cayo Coco, respectively (Fig. 4). These Δ_{pyr} values are consistent with near thermodynamic equilibrium fractionation as observed in *i*) MSR batch culture experiments characterised by low growth rate and csSRR (Leavitt *et al.*, 2013; Bradley *et al.*, 2016) and *ii*) natural environments (*e.g.*, Cadagno Lake; Canfield *et al.*, 2010). High $^{34}\varepsilon_{mic}$ has been observed in sulfate reducing strains only partially oxidising their carbon substrate and is sometimes associated with the degradation of carbohydrate components, including exopolymeric substances (EPS) (Sim *et al.*, 2011), which are abundant in microbialite-forming mats. Atexcac waters have a high dissolved organic carbon content (over 15 times that of the modern ocean) which can sustain MSR activity, while Cayo Coco harbours conspicuous suspended EPS-rich organic slimes (Bouton *et al.*, 2016). Despite abundant sulfate (at Cayo Coco) and organic matter, csSRR in these mats are intriguingly low and contrast with previous occurrences of high SRR in surface microbial mats (Canfield and Des Marais, 1993). Low csSRR and high S isotope fractionations in both lakes could be explained by the refractory nature of this organic matter (Bouton *et al.*, 2020; Gomes *et al.*, 2021). At the microbial mat scale, strong gradients of sulfate reduction within layered mats (Visscher *et al.*, 2000; Fike *et al.*, 2009; Pace *et al.*, 2018) have been attributed to small scale variations in csSRR and/or localised MSR micro-niches (Fike *et al.*, 2009; Gomes *et al.*, 2021). The observed laminations, which contain micropyrites, likely reflect local high density microbe spots, which can result from a more pronounced local distillation of $\delta^{34}S$ (Pasquier *et al.*, 2021). Alternatively, the composition of microbial consortia may affect the range of csSRR at the microbial mat scale (Bradley *et al.*, 2016), with guild diversity having opposite effects on trophic group functions, thus modulating csSRR (Bell *et al.*, 2005; Peter *et al.*, 2011).

Conclusions

Here, we have shown that the S isotope composition of framboids and micropyrites reflects sulfur cycling at the scale of the mat environment. While S isotope signatures in microbialite micropyrites are primarily controlled by MSR, they can also be influenced by oxidative sulfur cycling in high pH environments. Notably, microbialites growing at different dissolved sulfate concentrations and in marine versus lacustrine environments display similar micropyrite morphologies and comparable Δ_{pyr}. Such observations demonstrate that microbialites have the potential to record the isotopic fractionation associated with MSR irrespective of the depositional environment and sulfate level. Consequently, we propose that microbialite micropyrites can be used as a mineral signature for reconstructing past Earth surface and microbial environments, as already suggested for Archaean stromatolites (Marin-Carbonne *et al.*, 2018). In addition, this study clearly shows that caution should be used in reconstructing past environmental parameters, such as water body sulfate levels, from Δ_{pyr}. Finally, the respective influence of different electron donors, sulfate concentration, and non-actualistic microbial communities on the csSRR and associated sedimentary pyrites $\delta^{34}S$ remains to be explored in order to deepen our understanding of the evolutionary trajectory of biogeochemical sulfur cycling on Earth.

Author contributions

JMC, LR, SB and CT designed the study, KB, EV, CT and AB collected samples in the field. JMC, LR, MND and SE conducted the NanoSIMS analyses, CT and RH conducted the bulk S isotope analyses. JMC, MND, JA, AB, NZ and KB conducted the microscope observations. All authors have contributed to the data interpretation. JMC wrote the manuscript with important contributions of all co-authors.

Competing interests

Authors declare no competing interests.

Data and materials availability

All data is available in the main text or the supplementary materials.

Additional Information

Supplementary Information accompanies this letter at https://www.geochemicalperspectivesletters.org/article2209.

Acknowledgements

This research was supported through the European Research council (ERC) under the European Union's Horizon H2020 research and innovation programme (STROMATA grant agreement 759289). The NanoSIMS facility at the Museum National d'Histoire Naturelle in Paris was established by funds from the CNRS, region ile de France, Ministère délégué à l'enseignement et à la recherche and the Museum National d'Histoire Naturelle. We thank Kevin McKeegan and Jasmine Berg for their proofreading of the manuscript and for fruitful discussions.

Editor: Tanja Bosak

Cite this letter as: Marin-Carbonne, J., Decraene, M.-N., Havas, R., Remusat, L., Pasquier, V., Alléon, J., Zeyen, N., Bouton, A., Bernard, S., Escrig, S., Olivier, N., Vennin, E., Meibom, A., Benzerara, K., Thomazo, C. (2022) Early precipitated micropyrite in microbialites: A time capsule of microbial sulfur cycling. *Geochem. Persp. Let.* 21, 7–12. https://doi.org/10.7185/geochemlet.2209

References

Alleon, J., Bernard, S., Olivier, N., Thomazo, C., Marin-Carbonne, J. (2021) Inherited geochemical diversity of 3.4 Ga organic films from the Buck Reef Chert, South Africa. *Communications Earth & Environment* 2, 6. https://doi.org/10.1038/s43247-020-00066-7

Allwood, A.C., Grotzinger, J.P., Knoll, A.H., Burch, I.W., Anderson, M.S., Coleman, M.L., Kanik, I. (2009) Controls on development and diversity of Early Archean stromatolites. *Proceedings of the National Academy of Sciences* 106, 9548–9555. https://doi.org/10.1073/pnas.0903323106

Awramik, S.M. (1992) The history and significance of stromatolite. In: Schidlowski, M., Golubic, S., Kimberley, M.M., McKirdy, D.M., Trudinger, P.A. (Eds.) *Early organic evolution*. Springer, Berlin, 435–449. https://doi.org/10.1007/978-3-642-76884-2_34

Bell, T., Newman, J.A., Silverman, B.W., Turner, S.L., Lilley, A.K. (2005) The contribution of species richness and composition to bacterial services. *Nature* 436, 1157–1160. https://doi.org/10.1038/nature03891

Bouton, A., Vennin, E., Pace, A., Bourillot, R., Dupraz, C., Thomazo, C., Brayard, A., Désaubliaux, G., Visscher, P.T. (2016) External controls on the distribution, fabrics and mineralization of modern microbial mats in a coastal hypersaline lagoon, Cayo Coco (Cuba). *Sedimentology* 63, 972–1016. https://doi.org/10.1111/sed.12246

Bouton, A., Vennin, E., Thomazo, C., Mathieu, O., Garcia, F., Jaubert, M., Visscher, P. (2020) Microbial Origin of the Organic Matter Preserved in the Cayo Coco Lagoonal Network, Cuba. *Minerals* 10, 143. https://doi.org/10.3390/min10020143

Bradley, A.S., Leavitt, W.D., Schmidt, M., Knoll, A.H., Girguis, P.R., Johnston, D.T. (2016) Patterns of sulfur isotope fractionation during microbial sulfate reduction. *Geobiology* 14, 91–101. https://doi.org/10.1111/gbi.12149

Canfield, D.E., Des Marais, D.J. (1993) Biogeochemical cycles of carbon, sulfur, and free oxygen in a microbial mat. *Geochimica et Cosmochimica Acta* 57, 3971–3984. https://doi.org/10.1016/0016-7037(93)90347-Y

Canfield, D.E., Farquhar, J., Zerkle, A.L. (2010) High isotope fractionations during sulfate reduction in a low-sulfate euxinic ocean analog. *Geology* 38, 415–418. https://doi.org/10.1130/G30723.1

Fike, D.A., Finke, N., Zha, J., Blake, G., Hoehler, T.M., Orphan, V.J. (2009) The effect of sulfate concentration on (sub)millimeter-scale sulfide $\delta^{34}S$ in hypersaline cyanobacterial mats over the diurnal cycle. *Geochimica et Cosmochimica Acta* 73, 6187–6204. https://doi.org/10.1016/j.gca.2009.07.006

Fike, D.A., Gammon, C.L., Ziebis, W., Orphan, V.J. (2008) Micron-scale mapping of sulfur cycling across the oxycline of a cyanobacterial mat: a paired nanoSIMS and CARD-FISH approach. *The ISME Journal* 2, 749–759. https://doi.org/10.1038/ismej.2008.39

Fry, B., Ruf, W., Gest, H., Hayes, J.M. (1988) Sulfur isotope effects associated with oxidation of sulfide by O_2 in aqueous solution. *Chemical Geology: Isotope Geoscience section* 73, 205–210. https://doi.org/10.1016/0168-9622(88)90001-2

Goldhaber, M.B., Kaplan, I.R. (1980) Mechanisms of sulfur incorporation and isotope fractionation during early diagenesis in sediments of the Gulf of California. *Marine Chemistry* 9, 95–143. https://doi.org/10.1016/0304-4203(80)90063-8

Gomes, M.L., Fike, D.A., Bergmann, K.D., Jones, C., Knoll, A.H. (2018) Environmental insights from high-resolution (SIMS) sulfur isotope analyses of sulfides in Proterozoic microbialites with diverse mat textures. *Geobiology* 16, 17–34. https://doi.org/10.1111/gbi.12265

Gomes, M.L., Klatt, J.M., Dick, G.J., Grim, S.L., Rico, K.I., Medina, M., Ziebis, W., Kinsman-Costello, L., Sheldon, N.D., Fike, D.A. (2021) Sedimentary pyrite sulfur isotope compositions preserve signatures of the surface microbial mat environment in sediments underlying low-oxygen cyanobacterial mats. *Geobiology* 20, 60–78. https://doi.org/10.1111/gbi.12466

Javaux, E.J. (2019) Challenges in evidencing the earliest traces of life. *Nature* 572, 451–460. https://doi.org/10.1038/s41586-019-1436-4

Jørgensen, B.B., Findlay, A.J., Pallerin, A. (2019) The Biogeochemical Sulfur Cycle of Marine Sediments. *Frontiers in Microbiology* 10, 849. https://doi.org/10.3389/fmicb.2019.00849

Kamber, B.S., Whitehouse, M.J. (2007) Micro-scale sulphur isotope evidence for sulphur cycling in the late Archean shallow ocean. *Geobiology* 5, 5–17. https://doi.org/10.1111/j.1472-4669.2006.00091.x

Lang, X., Tang, W., Ma, H., Shen, B. (2020) Local environmental variation obscures the interpretation of pyrite sulfur isotope records. *Earth and Planetary Science Letters* 533, 116056. https://doi.org/10.1016/j.epsl.2019.116056

Leavitt, W.D., Halevy, I., Bradley, A.S., Johnston, D.T. (2013) Influence of sulfate reduction rates on the Phanerozoic sulfur isotope record. *Proceedings of the National Academy of Sciences* 110, 11244–11249. https://doi.org/10.1073/pnas.1218874110

Lepot, K. (2020) Signatures of early microbial life from the Archean (4 to 2.5 Ga) eon. *Earth-Science Reviews* 209, 103296. https://doi.org/10.1016/j.earscirev.2020.103296

Marin-Carbonne, J., Busigny, V., Miot, J., Rollion-Bard, C., Muller, E., Drabon, N., Jacob, D., Pont, S., Robyr, M., Bontognali, T.R.R., François, C., Reynaud, S., Van Zuilen, M., Philippot, P. (2020) In Situ Fe and S isotope analyses in pyrite from the 3.2 Ga Mendon Formation (Barberton Greenstone Belt, South Africa): Evidence for early microbial iron reduction. *Geobiology* 18, 306–325. https://doi.org/10.1111/gbi.12385

Marin-Carbonne, J., Remusat, L., Sforna, M.C., Thomazo, C., Cartigny, P., Philippot, P. (2018) Sulfur isotope's signal of nanopyrites enclosed in 2.7 Ga stromatolitic organic remains reveal microbial sulfate reduction. *Geobiology* 16, 121–138. https://doi.org/10.1111/gbi.12275

Pace, A., Bourillot, R., Bouton, A., Vennin, E., Braissant, O., Dupraz, C., Duteil, T., Bundeleva, I., Patrier, P., Galaup, S., Yokoyama, Y., Franceschi, M., Virgone, A., Visscher, P.T. (2018) Formation of stromatolite lamina at the interface of oxygenic-anoxygenic photosynthesis. *Geobiology* 16, 378–398. https://doi.org/10.1111/gbi.12281

Paerl, H.W., Pinckney, J.L. (1996) A mini-review of microbial consortia: their roles in aquatic production and biogeochemical cycling. *Microbial Ecology* 31, 225–247. https://doi.org/10.1007/BF00171569

Pasquier, V., Bryant, R.N., Fike, D.A., Halevy, I. (2021) Strong local, not global, controls on marine pyrite sulfur isotopes. *Science Advances* 7, eabb7403. https://doi.org/10.1126/sciadv.abb7403

Pellerin, A., Antler, G., Holm, S.A., Findlay, A.J., Crockford, P.W., Turchyn, A.V., Jørgensen, B.B., Finster, K. (2019) Large sulfur isotope fractionation by bacterial sulfide oxidation. *Science Advances* 5, eaaw1480. https://doi.org/10.1126/sciadv.aaw1480

Peter, H., Beier, S., Bertilsson, S., Lindström, E.S., Langenheder, S., Tranvik, L.J. (2011) Function-specific response to depletion of microbial diversity. *The ISME Journal* 5, 351–361. https://doi.org/10.1038/ismej.2010.119

Picard, A., Gartman, A., Clarke, D.R., Girguis, P.R. (2018) Sulfate-reducing bacteria influence the nucleation and growth of mackinawite and greigite. *Geochimica et Cosmochimica Acta* 220, 367–384. https://doi.org/10.1016/j.gca.2017.10.006

Raven, M.R., Sessions, A.L., Fischer, W.W., Adkins, J.F. (2016) Sedimentary pyrite $\delta^{34}S$ differs from porewater sulfide in Santa Barbara Basin: Proposed role of organic sulfur. *Geochimica et Cosmochimica Acta* 186, 120–134. https://doi.org/10.1016/j.gca.2016.04.037

Reid, R.P., Visscher, P.T., Decho, A.W., Stolz, J.F., Bebout, B.M., Dupraz, C., Macintyre, I.G., Paerl, H.W., Pinckney, J.L., Prufert-Bebout, L., Steppe, T.F., DesMarais, D.J. (2000) The role of microbes in accretion, lamination and early lithification of modern marine stromatolites. *Nature* 406, 989–992. https://doi.org/10.1038/35023158

Shen, Y., Farquhar, J., Masterson, A., Kaufman, A.J., Buick, R. (2009) Evaluating the role of microbial sulfate reduction in the early Archean using quadruple isotope systematics. *Earth and Planetary Science Letters* 279, 383–391. https://doi.org/10.1016/j.epsl.2009.01.018

Shen, Y., Buick, R. (2004). The antiquity of microbial sulfate reduction. *Earth-Science Reviews* 64, 243–272. https://doi.org/10.1016/S0012-8252(03)00054-0

Sim, M.S., Ono, S., Donovan, K., Templer, S.P., Bosak, T. (2011) Effect of electron donors on the fractionation of sulfur isotopes by a marine *Desulfovibrio* sp. *Geochimica et Cosmochimica Acta* 75, 4244–4259. https://doi.org/10.1016/j.gca.2011.05.021

Slotznick, S.P., Johnson, J.E., Rasmussen, B., Raub, T.D., Webb, S.M., Zi, J.-W., Kirschvink, J.L., Fischer, W.W. (2022) Reexamination of 2.5-Ga "whiff" of oxygen interval points to anoxic ocean before GOE. *Science Advances* 8, eabj7190. https://doi.org/10.1126/sciadv.abj7190

Visscher, P.T., Reid, R.P., Bebout, B.M. (2000) Microscale observations of sulfate reduction: Correlation of microbial activity with lithified micritic laminae in modern marine stromatolites. *Geology* 28, 919–922. https://doi.org/10.1130/0091-7613(2000)28<919:MOOSRC>2.0.CO;2

Williford, K.H., Van Kranendonk, M.J., Ushikubo, T., Kozdon, R., Valley, J.W. (2011) Constraining atmospheric oxygen and seawater sulfate concentrations during Paleoproterozoic glaciation: In situ sulfur three-isotope microanalysis of pyrite from the Turee Creek Group, Western Australia. *Geochimica et Cosmochimica Acta* 75, 5686–5705. https://doi.org/10.1016/j.gca.2011.07.010

Zeyen, N., Benzerara, K., Beyssac, O., Daval, D., Muller, E., Thomazo, C., Tavera, R., López-García, P., Moreira, D., Duprat, E. (2021) Integrative analysis of the mineralogical and chemical composition of modern microbialites from ten Mexican lakes: What do we learn about their formation. *Geochimica et Cosmochimica Acta* 305, 148–184. https://doi.org/10.1016/j.gca.2021.04.030